

MULTI-SCALE 3D IMAGING OF CARBON FIBRE LAMINATE IMPACT AND COMPRESSION AFTER IMPACT DAMAGE USING COMPUTED TOMOGRAPHY AND LAMINOGRAPHY

D. Bull^{1*}, L. Helfen², I. Sinclair¹, S.M. Spearing¹

¹Materials Research Group, Faculty of Engineering and the Environment, University of Southampton,
Southampton, United Kingdom

²ANKA / Institute for Synchrotron Radiation, Forschungszentrum Karlsruhe, Germany

*daniel.bull@soton.ac.uk

Keywords: impact damage, compression after impact, computed tomography, laminography

Abstract

3D X-ray computed tomography (CT) was used to study the effects of particle toughening within unidirectional carbon fibre reinforced polymer (CFRP) materials subjected to impact damage, followed by ex situ CT of compression after impact (CAI) tests at incremental loads. A multi-scale approach utilizing synchrotron radiation CT and laminography was used to study the damage micro-mechanisms of impact-loaded specimens, and micro-focus CT (μ CT) assessed damage at meso- and macro-scopic levels. For the ex situ compression after impact testing, plates were CT scanned after progressively larger compressive loads were applied. Particle toughening processes were observed, with damage growth and micro-buckling events being captured close to the final failure in the CAI test.

1 Introduction

Due to their high strength and stiffness to weight ratios, CFRP materials are increasingly used on primary and secondary aircraft structures. One of the concerns however is their poor resistance to impact damage, which has a direct effect on the residual compressive strength of the material. Due to the level of threat of impact throughout the service life of the aircraft, this poses a serious problem to aircraft operators and manufactures [1].

The detectability of impact damage becomes problematic at the barely visible impact damage (BVID) level at which point significant internal damage exists beneath the surface of the material [2]. Whilst this internal damage can be detected with ultrasonic techniques, damage can go unnoticed for some time in between service inspections [3]. This calls for better damage resistant and damage tolerant materials to be developed; which require a better understanding of the damage behavior after an impact event and subsequently how this damage contributes to final compressive failure.

The development of CFRP structures has hitherto been largely empirically-based. Whilst experimental mechanics and instrumented testing can identify materials with better properties, the key to developing better materials is to study the internal damage mechanisms

caused by impact and their role in influencing the residual strength under in-plane compression. Current techniques include ultrasonic C-scan and optical methods however these have their limitations and in particular they are restricted to generating two dimensional (2D) images of damage [4, 5]. Considering the three-dimensional (3D) micro-level damage behavior and the various types of damage modes within the material, 3D X-ray tomography and laminography offers the ability to carry out the necessary 3D damage assessments [6-11].

There is an intrinsic tradeoff between the field of view and voxel resolution of conventional CT scanning and in this work a multi-scale approach was undertaken. To achieve the highest possible resolution, synchrotron radiation CT (SRCT) and laminography (SRCL) allows damage micro-mechanisms to be captured, and in previous studies, this has worked well [7, 8]. To study the overall macro-level damage characteristics, a combination of multiple scans at a lower resolution can be used to provide a larger field of view. This is typically up to 10x10x10mm at 5 μ m voxel resolution using a 2000x2000 pixel detector. The voxel resolution used is often greater than the finest damage features, such as near-tip crack openings, however the partial volume effect can be exploited; allowing sub-voxel features to be detected with a reduction in contrast between crack and material [10]. Contrast may also be increased with the use of contrast agents, such as iodine-containing solutions; however this requires interconnections of the damage to allow full penetration of the dye [10].

Due to the high aspect ratio of plates, there are large variations in X-ray path length as the sample rotates as shown in Figure 1(a); this leads to variable attenuations in the radiograph data. To allow for the highest possible resolution and fidelity of CT scan, regions of interest of more isotropic cross-section (e.g. circle or square) are required to be physically removed from the larger, original test specimen, rendering the technique destructive. Laminography can avoid such issues in high aspect ratio planar objects by tilting the rotation axis shown in Figure 1(b) [9]. This maintains an essentially constant X-ray path length through the object and has successfully been used in previous studies on composite material [7].

There are two main purposes to this work; the first serves to illustrate the feasibility of these techniques to assess impact damage and its subsequent influence on final failure under compression; the second aim is to gain a better understanding in the role of particle toughening within the CFRP material. A combination of 3D multi-scale imaging and *ex situ* CAI experiments qualitatively shows damage interactions and progression from an impact event, leading up to final compressive failure. Direct comparisons between non-particle and particle toughened systems will be assessed.

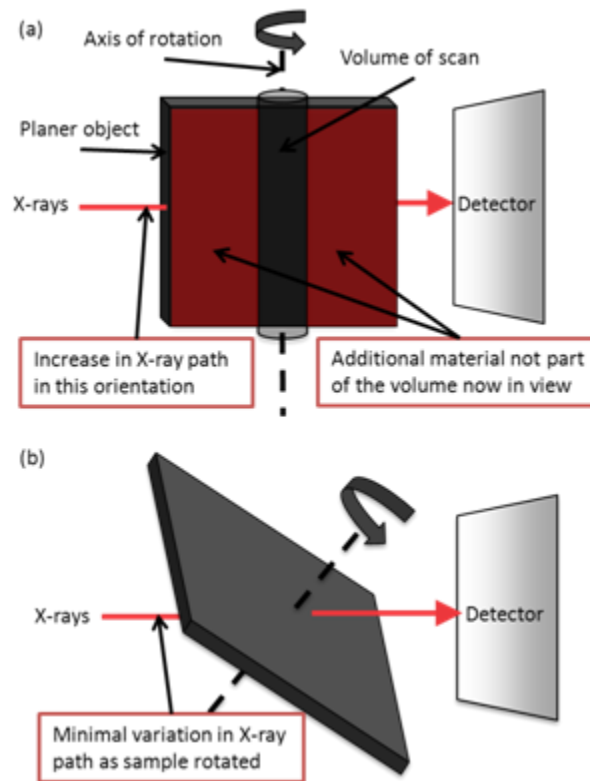


Figure 1. Schematic comparison of geometries associated with: (a) SRCT and (b) SRCL

2 Materials and testing methods

2.1 Materials

Two geometries of CFRP material were used. For studying impact damage, an 8 ply sample with a $[-45, 90, +45, 0]_S$ layup was used, measuring $80 \times 80 \times \sim 1$ mm. The 1mm thickness was chosen in keeping with previous laminography studies. To study the effect of CAI, ASTM standard samples $150 \times 100 \times \sim 4.5$ mm were used with a $[-45, 90, +45, 0]_{3S}$ layup. Samples were C-scanned to check for defects.

2.2 Mechanical drop tower testing

A drop tower with a 4.9kg, 16mm diameter hemispherical striker was used. The height of the drop was adjusted to achieve the desired impact energy. Specimens were loosely clamped onto a base plate; this contained a 60mm diameter hole for the 1mm specimens, and a rectangular window measuring 125×75 mm for the 4.5mm thick specimens. Samples used for impact damage assessment were impacted to achieve a damage radius of approximately 5mm when measured by C-scan. This required toughened and non-toughened specimens to be impacted at 1.3J and 0.6J respectively. Preparation of these impacted samples prior to high resolution CT scanning involved cutting out regions of interest approximately 4.5mm wide across the height of the sample.

2.3 *Ex situ* CAI CT testing

Samples used for this experiment were impacted at 30J. These were placed in an anti-buckling device and progressively loaded in compression by incremental load steps, with the first step occurring when audible damage was detected. In between steps, the sample was taken out and scanned on the μ CT scanner.

2.3 3D X-ray computed tomography

μ CT scans were undertaken at the μ -VIS X-ray Imaging facility at the University of Southampton, UK. SRCT and SRCL scans were carried out using beamline ID19 at the European Synchrotron Radiation Facility (ESRF), France.

2.3.1 Micro-focus CT

There are three roles that μ CT served in this work. The first was to identify regions of interest in samples for SRCT work. The second role was to capture the entire damaged region combining a stack of multiple ‘matchsticks’ extracted from damage regions, with the multiple CT dataset then stitched back together shown in Figure 2. Finally for the *ex situ* CAI work, whole plates were imaged in the CT scanner (intact), with the direction of loading parallel to the rotation axis.

‘Matchstick’ specimens (approximately 50x4x2mm) were scanned at a voxel resolution of 4.3 μ m at 80kV and 80 μ A over 2001 projections. Local scans of the plates were carried out for the *ex situ* CAI work, this was done at the maximum voxel resolution determined by the clearance distance between the sample and the target giving a voxel resolution of 12.5 μ m, using a tube voltage of 105kV.

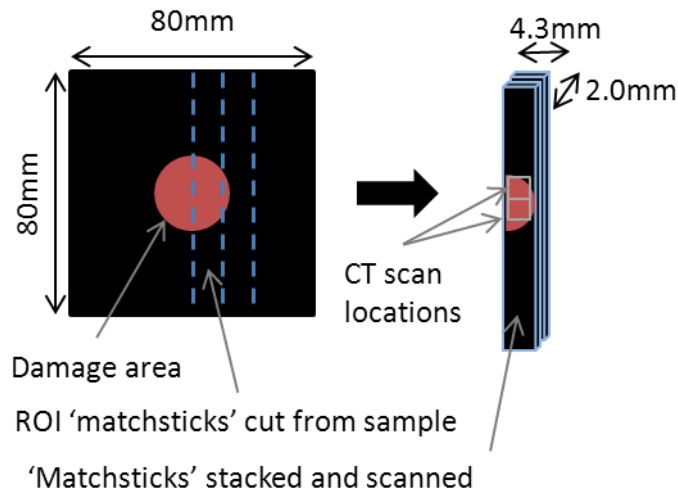


Figure 2. ‘Matchstick’ sample preparation across damage areas for CT analysis

2.3.2 SRCT

SRCT was performed at the European Synchrotron Radiation Facility (ESRF), Grenoble. Regions of interest identified from the μ CT work were scanned at a voxel resolution of 1.4 μ m.

2.3.3 SRCL

A second set of impacted specimens were used to carry out SRCL work at a $0.7\mu\text{m}$ voxel resolution. Local regions of interest were scanned within a quarter of the damage area identified from ultrasonic C-scan analysis, see Figure 3.

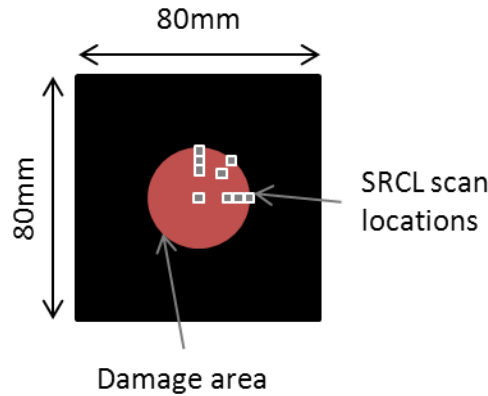


Figure 3. Regions of interest imaged via SRCL.

2.4 Visualisation

Reconstructed volumes were analysed using VG Studio Max. SRCT volumes were concatenated together from multiple scans to form a larger volume. Different crack modes from SRCT and SRCL were identified and segmented semi-automatically using a region-growing tool to form a 3D representation of damage. Additionally, 2D cross-sectional slices of damage at different orthogonal planes were assessed to confirm reasonable representation in the 3D segmentations.

3 Results and Discussion

3.1 Impact damage assessment

After stitching together multiple μCT scans, segmentation revealed the extent of impact damage within the material, as shown in Figure 5. A distinct conical pattern of damage surrounding the impact region is shown, with clear interactions of delaminations occurring between matrix cracks, consistent with matrix cracking having occurred first, initiating delaminations at the interply regions, as suggested in previous work [4, 5]. Comparisons between toughened and non-toughened systems reveal similar damage behavior and extent of intralaminar damage, however a significant reduction to the extent of delaminations was revealed in the particle systems, indicative of the distinctive role of toughening particles in the interply region.

SRCL facilitated high resolution non-destructive 3D analysis of impacted material, revealing internal damage down to the micro-level, comparable to SRCT. A direct comparison between the two material systems is shown in Figure 6. It is evident that particle toughened system incorporates a thicker resin rich region at the ply interface ($\sim 30\mu\text{m}$ thickness). Additionally, these particles lead to local coarser echelon crack geometry, with large bridging ligaments in the region of $30\mu\text{m}$ (confirmed by SRCT also).

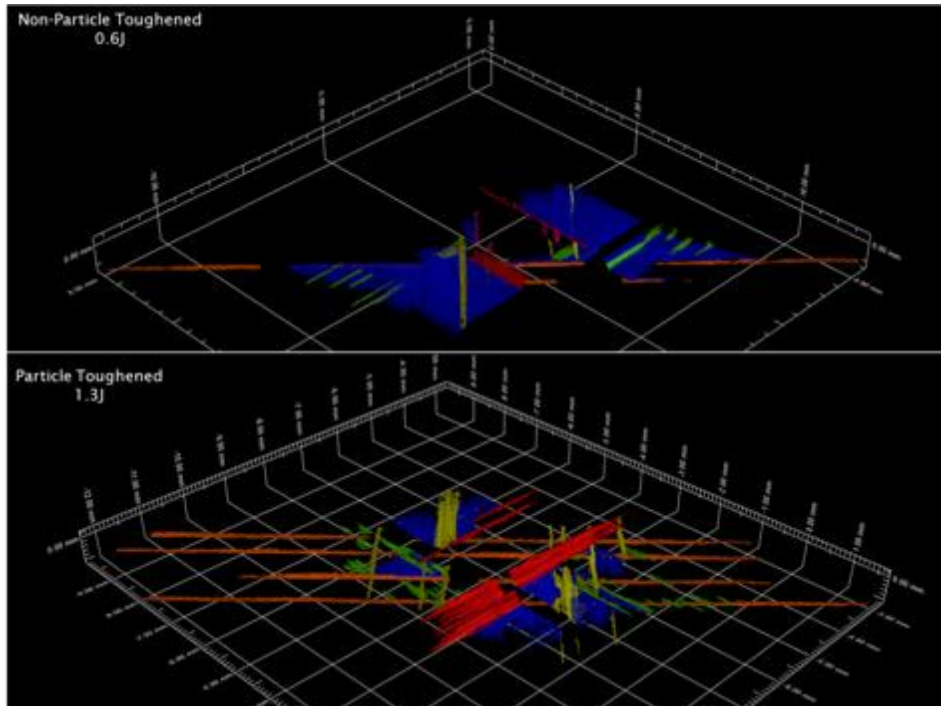


Figure 5. 3D segmentation of impact damage comparing non-particle and particle toughened material. Blue highlights delaminations; other colors represent matrix cracks occurring on different plies.

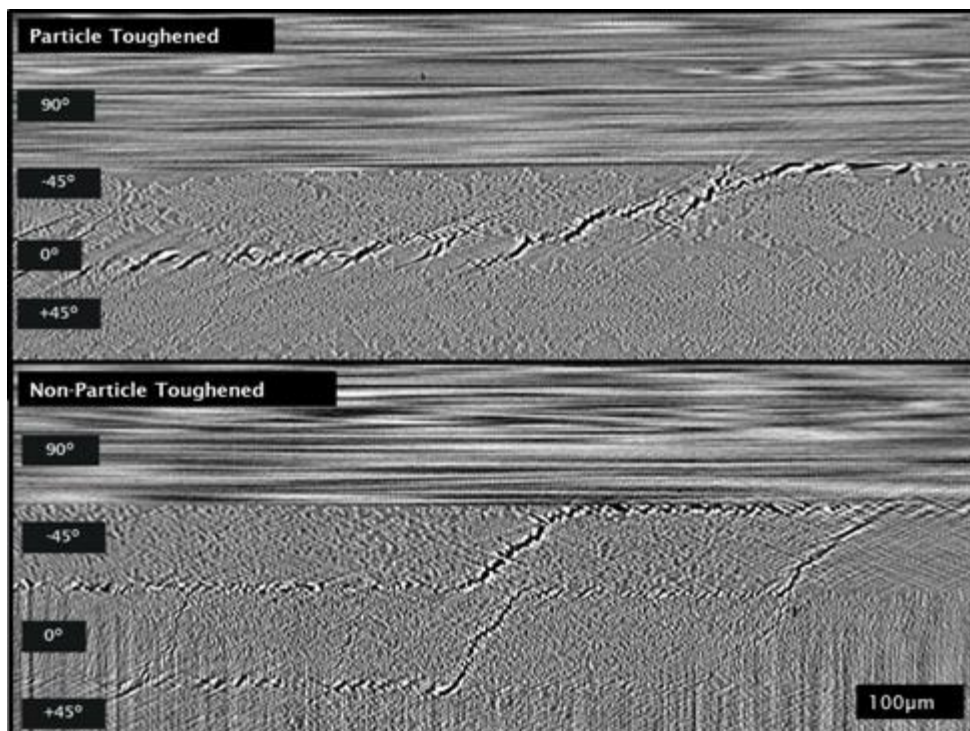


Figure 6. SRCL cross section showing a comparison of the delamination micromechanisms between a particle toughened and a non-particle toughened system

3.2 *Ex situ* CAI damage progression

By utilizing the μ CT scanner within a program of interrupted CAI tests, damage progression has been monitored as a compressive load is applied at increasing levels. Preliminary work revealed evidence of crack growth and increased crack openings at 99% of the critical failure load (see Figure 7), consistent with the assertion that the primary mechanism of failure in compression after impact is local buckling of the impacted region, rather than extensive subcritical damage growth. Early stages of micro-buckling were observed occurring internally on the load bearing 0° plies and is shown in Figure 8 for the toughened systems. [12-14].

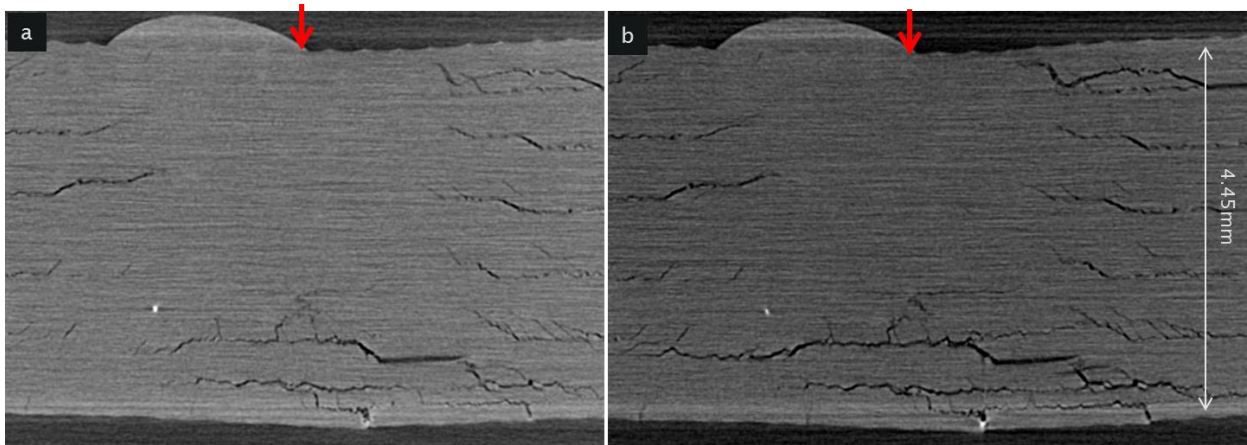


Figure 7. Through-thickness μ CT slice, with arrow indicating impact location for a) after impact and b) after a 99% of failure load for a particle toughened system

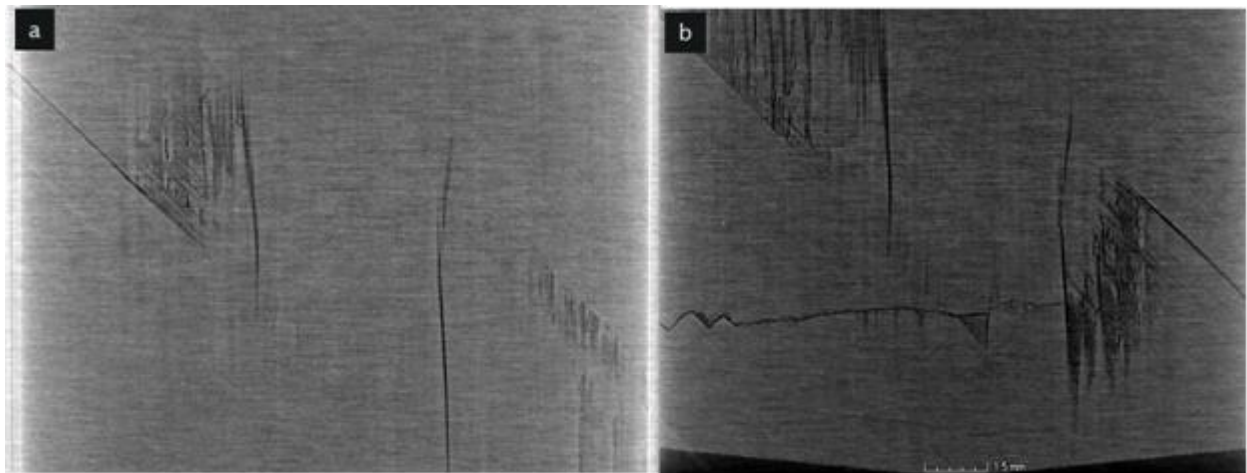


Figure 8. In-plane μ CT slice showing a $0^\circ/45^\circ$ ply interface a) damage after impact and b) micro-buckling occurring at 99% of failure load for a particle toughened system

4 Conclusions

μ CT, SRCT and SRCL was successfully used to capture damage conditions associated with CAI at multiple-scales.. Segmentation of the μ CT scans reveals a similar extent of matrix cracking with particle and non-particle toughened systems, however reductions in delaminations were observed. SRCL showed micromechanical differences between toughened and non-toughened material systems, where the effects of particle toughening at

the ply interfaces were seen crack bridging and blunting. μ CT scans of interrupted CAI tests revealed damage propagation and micro-buckling events occurring at near-critical failure loads (99% of maximum).

5 Acknowledgements

Special thanks for the ESRF for use of their facilities with the synchrotron radiation CT and synchrotron radiation laminography work. Additional thanks goes to Cytec for their sponsorship and supply of materials used in this project.

References

- [1] Soutis, C., *Carbon fiber reinforced plastics in aircraft construction*. Materials Science and Engineering a-Structural Materials Properties Microstructure and Processing, 2005. **412**(1-2): p. 171-176.
- [2] Polimeno, U. and M. Meo, *Detecting barely visible impact damage detection on aircraft composites structures*. Composite Structures, 2009. **91**(4): p. 398-402.
- [3] Sanchu-Saez, S., et al., *Compression after impact of thin composite laminates*. Composites Science and Technology, 2005. **65**(13): p. 1911-1919.
- [4] Aymerich, F. and S. Meili, *Ultrasonic evaluation of matrix damage in impacted composite laminates*. Composites Part B-Engineering, 2000. **31**(1): p. 1-6.
- [5] Shyr, T.W. and Y.H. Pan, *Impact resistance and damage characteristics of composite laminates*. Composite Structures, 2003. **62**(2): p. 193-203.
- [6] Wright, P., et al., *Ultra high resolution computed tomography of damage in notched carbon fiber-epoxy composites*. Journal of Composite Materials, 2008. **42**(19): p. 1993-2002.
- [7] Moffat, A.J., et al., *In situ synchrotron computed laminography of damage in carbon fibre-epoxy [90/0](s) laminates*. Scripta Materialia, 2010. **62**(2): p. 97-100.
- [8] Moffat, A.J., et al., *Micromechanisms of damage in 0 degrees splits in a [90/0](s) composite material using synchrotron radiation computed tomography*. Scripta Materialia, 2008. **59**(10): p. 1043-1046.
- [9] Helfen, L., et al., *Synchrotron-radiation computed laminography for high-resolution three-dimensional imaging of flat devices*. Physica Status Solidi a-Applications and Materials Science, 2007. **204**(8): p. 2760-2765.
- [10] Schilling, P.J., et al., *X-ray computed microtomography of internal damage in fiber reinforced polymer matrix composites*. Composites Science and Technology, 2005. **65**(14): p. 2071-2078.
- [11] Bull, D.J., et al. *Composite laminate impact damage assessment by high resolution 3D X-ray tomography and laminography*. in *18th international conference on composite materials*. 2011. Jeju, S. Korea.
- [12] Ward, S.H. and H. Razi, *Effect of thickness on the compression residual strength of notched carbon fiber/epoxy composites*. Technology Transfer in a Global Community, 1996. **28**: p. 177-188.
- [13] Chen, P.H., Z. Shen, and J.Y. Wang, *A new method for compression after impact strength prediction of composite laminates*. Journal of Composite Materials, 2002. **36**(5): p. 589-610.
- [14] Soutis, C., *Measurement of the Static Compressive Strength of Carbon-Fiber Epoxy Laminates*. Composites Science and Technology, 1991. **42**(4): p. 373-392.